J Fluoresc (2013) 23:147–157
DOI 10.1007/s10895-012-1128-z

ORIGINAL PAPER

Comparison of FÖrster-Resonance-Energy-Transfer Acceptors for Tryptophan and Tyrosine Residues in Native Proteins as Donors

Yi zhang · Xiaolan Yang · Lin Liu · Zuexia Huang · Jun Pu · Gaobo Long · Ling Zhang · Dong Liu · Bangtian Xu · Juan Liao · Fei Liao

Received: 7 July 2012 / Accepted: 5 September 2012 / Published online: 22 September 2012

Abstract Homogenous bioaffinity analysis with tryptophan/tyrosine residues in native proteins as FÖrster-resonance-energy-transfer (FRET) donors is feasible when suitable fluorophors can act as FRET acceptors in ligands (FRET probes) and FRET efficiency in complexes of proteins and FRET probes is high enough. In complexes of proteins and FRET probes, suitable acceptors should have excitation peaks around 335 nm and high rotation freedom, are preferred to have sufficient quantum yields and excitation valleys around 280 nm. In protein binding sites mimicked with mixtures of neutral phosphate buffer and organic solvents, quantum yields of candidate acceptors are altered inconsistently but their excitation peaks show tiny changes. Fluorophores as acceptors in such FRET probes are buried inside glutathione-S-transferase and have low rotation freedom, but are localized on streptavidin surface and display high rotation freedom; FRET efficiency in complexes of streptavidin and its FRET probes is much stronger than that in complexes of glutathione-S-transferase and its FRET probes. Specially, the quantum yield is about 0.70 for free 1-naphthylamine probe in neutral phosphate buffer, about 0.50 for 1-naphthylamine probe bound by streptavidin, and about 0.15 for that bound by glutathione-S-transferase. The quantum yield is about 0.06 for free dansylamide probe, about 0.11 for dansylamide probe bound by streptavidin and about 0.27 for that bound by glutathione-S-transferase. Therefore, 1-naphthylamine and dansylamide are effective acceptors when they localize on surfaces of complexes of proteins and FRET probes.

Keywords FÖrster-resonance-energy-transfer · Acceptors · Tryptophan residues · Homogeneous bioaffinity analysis · Quantum yield · Excitation peak

Introduction

Homogenous bioaffinity analyses are important for estimating both affinities of candidate ligands and quantities of ligands or proteins in mixture samples [1–7]; they usually employ FÖrster-resonance-energy-transfer (FRET) with a donor and a paired acceptor whose excitation peak overlaps the emission peak of the donor [8–16]. For such analyses, proteins are frequently labeled with fluorophores to act as donors/acceptors while fluorescent ligands are used as the counterparts to exert FRET in their complexes. However, the labeling of proteins with fluorophores may alter their functions and cause false results. In fact, common proteins contain tryptophan and/or tyrosine residues and exhibit emission peaks around 335 nm under the excitation around 280 nm [16–21]; tryptophan and tyrosine residues in native proteins can thus act as intrinsic donors to carry out homogenous bioaffinity analysis when fluorescent ligands bearing excitation peaks around 335 nm are made available to act as both acceptors and FRET probes. This new type of homogeneous bioaffinity analysis is proven to be effective to

Yi zhang and Xiaolan Yang contributed equally to this work.

Y. zhang · X. Yang · L. Liu · Z. Huang · J. Pu · G. Long · L. Zhang · D. Liu · B. Xu · J. Liao · F. Liao (✉)
Unit for analytical probes and protein biotechnology, Key laboratory of medical laboratory diagnostics of the Education Ministry, College of Laboratory Medicine, Chongqing Medical University,
Chongqing 400016, China
e-mail: liaofeish@yahoo.com

F. Liao
e-mail: liaofeish@cqmu.edu.cn

some native proteins [19–21]. Therefore, the strategies to design such FRET probes should be established while the universal applicability of this new method still needs investigations.

The conjugation of non-fluorescent moieties bound by proteins with fluorophores suitable as the acceptors for tryptophan and tyrosine residues in native proteins can be a general strategy to design FRET probes [22–24]. In practice of this new method, the changes of fluorescence of proteins or FRET probes in reaction solutions under the excitation around 280 nm can be measured. FRET is sensitive to changes of distance between a donor and its paired acceptor and only fluorescence of aromatic residues close to binding sites is quenched by the bound FRET probes. The assay of protein fluorescence thus suffers high background and low sensitivity. As an alternative, the fluorescence of a FRET probe under the excitation around 280 nm can be quantified providing, (a) the emission of the FRET probe under the excitation around 335 nm is much higher than that under the excitation around 280 nm, and (b) the quantum yield of the bound FRET probe is high enough. However, acceptors in FRET probes can be buried inside protein binding sites, or else be localized on protein surfaces; protein binding sites are non-aqueous and quantum yields of fluorophores are sensitive to changes of environments. As a result, an acceptor in FRET probes of different proteins may exhibit different quantum yields due to different binding modes. More importantly, reasonable FRET efficiency in complexes with proteins requires an angular factor that is usually approximated to be about 2/3 when the acceptors and/or donors display random orientation. For this new method, therefore, acceptors or donors in complexes with proteins should have sufficient rotation freedom [16]. An acceptor buried inside protein binding sites should have low rotation freedom while tryptophan and tyrosine residues inevitably exhibit restricted rotation; such low rotation freedom of an acceptor and donors inevitably reduces the FRET efficiency in the complexes with proteins and thus devalues this new method. Furthermore, suitable fluorophores in FRET probes should have small sizes for reasonable affinities of the probes to proteins. Hence, fluorophores as the unique acceptors in FRET probes should be rigorously selected and effects of binding modes of acceptors in FRET probes on reliability of this new method should be carefully investigated.

Derivatives of acridinine, 1-naphthylamine, coumarin, and dansylamide have excitation peaks close to 335 nm and are candidate acceptors (Fig. 1). Herein, to facilitate the design of FRET probes and the selection of candidate fluorophores as suitable acceptors, we compare their properties relevant to the sensitivity of this new type of homogenous bioaffinity analysis and further examine effects of binding modes of acceptors on the reliability of this new method.

Materials and Methods

Materials, Reagents, and Apparatus

Dansyl chloride (DNS-Cl), *N*-(1-naphthyl)-ethylenediamine (NEDA) hydrochloride, 4-methyl-7-hydroxycoumarin, 4-(diethylamino)-salisylaldehyde, acridine-9-carboxyl acid and 9-methylacridine were from Alfa Aesar. Glutathione-Sepharose 4B was from Sigma-Aldrich. Streptavidin (SAV) was from Promega. Other chemicals were domestic analytical reagents. Mapada UV 1600 PC spectrophotometer was

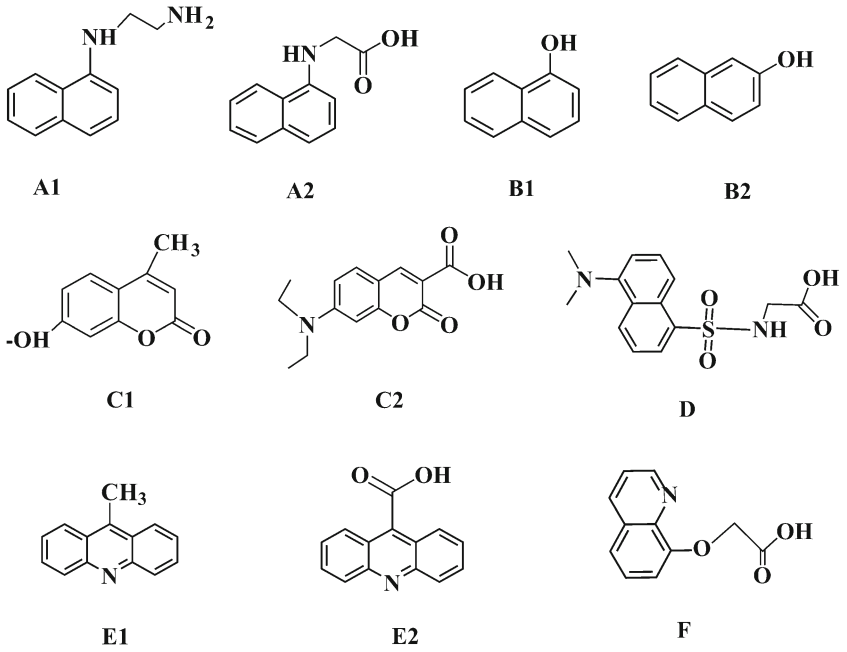

Fig. 1 Structure of tested fluorophores

used. Agilent Cary Eclipse fluorospectrometer was used with the excitation and emission slits of 10 nm, unless otherwise stated. Structures were determined by electrospray-ionization high-resolution-mass-spectrometry (ESI-HRMS) on API QSTAR LC-Q-TOF, and by NMR data of ^{1}H and ^{13}C on DRX 500 M Hz NMR spectrometer (Kunming Institute of Botany, Chinese Academy of Sciences, Yunnan 650224).

Preparation of Glutathione-S-Transferase (GST) and Estimation of Kinetic Parameters

Fresh porcine liver (200 g) was homogenized with 400 ml 10 mM Tris–HCl buffer at pH 6.8 containing 0.25 M sucrose, 1.0 mM EDTA, and 0.50 mM dithiothreitol. After centrifugation at 10,000 rpm for 30 min, the supernatant was fractionated with ammonium sulfate between 45 % and 85 % saturation. The resulting precipitates were collected by centrifugation, and dissolved in 50 ml Tris–HCl buffer (10 mM, pH 8.0) for dialysis against several changes of 500 ml distilled water. The supernatant after centrifugation at 10,000 rpm for 30 min was loaded for DEAE-cellulose (DE52) chromatography using the equilibrating buffer of 10 mM Tris–HCl buffer at pH 8.0. After removal of loosely-bound proteins with the equilibrating buffer, bound GST was eluted out with a linear gradient of NaCl from 0.10 to 0.40 M in 10 mM Tris–HCl buffer at pH 8.0. The pooled active portions were loaded on GSH-Sepharose 4B affinity column equilibrated with buffer A (10 mM sodium phosphate at pH 7.3 plus 0.14 M NaCl and 2.7 mM KCl). Unbound proteins were washed out with buffer A while bound proteins were eluted with buffer B (pH 8.0, 50 mM Tris–HCl contains 10.0 mM glutathione). Active portions were collected and stored below −15 °C. Before use, the preparation was dialyzed at 4 °C against 10 mM sodium phosphate buffer at pH 7.0. Native PAGE analysis supported homogenecity of the preparation. GST activity was determined with 1.0 mM GSH and 1.0 mM 2,4-dinitrochlorobenzene at 25 °C by absorbance at 340 nm with absorptivity of 9.6 $(mM{\cdot}cm)^{-1}$. The prepared GST accounted for nearly 30 % of the total activity of GST in pig liver homogenates. For estimating kinetic parameters, glutathione and 2,4-dinitrochlorobenzene concentrations were varied from 0.05 to over 2.0 mM; initial rates were analyzed by Lineweaver-Burk plot according to GST kinetics [25, 26].

Preparation of Fluorophores and FRET Probes

1-Naphthylamine Probes

(a) *N*-(biotinyl)-*N*′-(1-naphthyl)-ethylenediamine (BNEDA) were prepared as described previously [19, 20, 27, 28]. (b) *N*-(1-naphthyl)-glycine was prepared with 1-naphthylamine (10.0 g) and chloroacetic acid (4.0 g) in 20 ml NaOH solution (0.10 M) [29]. (c) cyclohexanylcarboxylic acid was activated in chloroform with *N*-hydroxysuccinimide and dicylcohexanylcarbadiimide for 3 h at 25 °C; after the removal of precipitates, NEDA at 1:1 molar ratio was directly added for further reaction of 3 h in dark. The solution was repetitively washed with 0.1 mM HCl, water and 1.0 M NaOH; the removal of solvents finally gave *N*-(1-naphthyl)-*N*′-cyclohexanylcarbonyl-ethylenediamine (NCHEDA). NCHEDA was verified by ESI-HRMS with molecular weight (MW) of 297.4136 Dalton while the calculated MW for its monocation derivatised from the complexing with single $^{1}H^{+}$ was 297.4142 Dalton.

Dansylamide Probes

(a) DNS-Cl was reacted with ethylenediamine at 1:10 molar ratio in dichloromethane to prepare mono-dansylated ethylenediamine followed by purification via silica chromatography. *N*-biotinyl-*N*′-dansyl-ethylenediamine (BDEDA) was prepared with mono-dansylated ethylenediamine as described previously [20], and stored below −20 °C till use. (b) Dansylglycine was prepared with DNS-Cl in THF and glycine in 0.10 M NaOH. After the concentration of reaction mixture, dansylglycine was purified by precipitation with HCl at pH 4.5 and wash with water. (c) DNS-Cl and 1,3-propanyldiamine (2.2:1) were mixed in chloroform : pyridine (5:1) under stirring at 25 °C. After reaction for 3 h, solvents were removed under reduced pressure and the residuals were washed vigorously and repetitively with 0.10 M NaOH and 0.10 mM HCl. The green residuals were dissolved in dichloromethane, washed again with 0.10 M NaOH, water and 0.10 mM HCl repetitively, and dried over Na_2SO_4. The removal of solvents gave *N*,*N*′-didansyl-1,3-propanyldiamine (DDPDA). DDPDA was verified by HRMS with molecular weight of 541.7009 Dalton while the calculated MW for its monocation derivatised from the complexing with single $^{1}H^{+}$ was 541.7012 Dalton.

Acridine Probes

Acridine-9-carboxylic acid (0.4 g) was refluxed in 12.0 ml dichlorosulfoxide for 2 h; after the removal of solvents, acridine-9-acylchloride was obtained and dissolved in 10.0 ml chloroform. This acylchloride solution was added to 3.0 ml ethylenediamine in 50 ml chloroform, and the resulting solution was refluxed for 3 h. To the residuals after removal of solvents, 5 ml 0.5 M NaOH solution was added and the collected precipitates were purified via chromatography to give *N*-(aridinyl-9-carboxyl)-ethylenediamine. In 30 ml THF solution of 0.3 g *N*-(aridinyl-9-carboxyl)-ethylenediamine, 150 mg active ester of biotin in THF was added for reaction at room temperature in dark for 3 h. After the

removal of solvents, the concentrated residuals in methanol were purified via chromatography to give *N*-(biotinyl)-*N*′-(acridine-9-carbonyl)-ethylenediamine (BACEDA) for storage below −20 °C. ESI-HRMS of BACEDA gave only two principal peaks, one with MW of 492.2068 Dalton (the calculated MW for its monocation derivatised from the complexing with single $^{1}H^{+}$ was 492.2063) and the other with MW of 514.1889 Dalton (the calculated MW for its monocation derivatised from the complexing with single $^{23}Na^{+}$ was 514.1883 Dalton). NMR data also supported the expected structure of BACEDA (data not given).

Nonfluorescent Biotin Derivatives

They were prepared as previously described [20].

Coumarin Fluorophores

4-diethylamino-salicylaldehyde (1.4 g), diethylmalonate (1.3 g), piperidine (0.1 ml) and acetic acid (0.2 ml) were mixed in 20 ml n-BuOH; the mixture was refluxed for 12 h [30]. Orange solids were formed after cooling to room temperature. The solids were recovered, washed with *n*-BuOH and dried in vacuum (~1.5 g, ~90 %).

Fluorescence Properties and Quantum Yields

All samples were used in 10 mM sodium phosphate buffer at pH 7.0, unless otherwise stated. Fluorescence signals and spectra were recorded routinely at room temperature. To quantify quantum yield, quinine in 0.50 M sulfuric acid was used as the reference with a putative quantum yield of 0.58. All fluorophores were excited at 325 nm to record their emission spectra, unless otherwise stated. Concentrations of fluorophores were adjusted for absorbance below 0.030 at 325 nm. Signals from buffer and Raman scattering were corrected. Emission from 350 nm to that equal to the emission peak (λ_{em}) plus 100 nm was integrated. Quantum yield is calculated considering their integrated signals and their absorbance at the same excitation wavelength [16].

Docking of FRET Probes to GST

Molegro Virtual Docking (V2011.5.0 on Windows XP) was used. Structure models of FRET probes were generated with ACDfree 11.0 and saved as .mol2 files. The structure mode of porcine liver GST π was from Protein DataBank (ID: 3gss.pdb). Water molecules and the bound ligands were removed manually from the crystal structure. The selected region of the active site covered the whole binding cleft including the interface of the other interacting subunit, and the diameter of active site was preset at 1.2 nm. Tryptophan and tyrosine residues in the active site were displayed. Coordinates of complexes were saved for analysis by Pymol (v 11.0).

Estimation of Relative Affinity

The procedure and equation to calculate relative affinity of a nonfluorescent candidate ligand against an analytical FRET probe were as those described previously [20]. Relative affinities were from assays in duplicate with coefficients of variation below 15 %. Quantum yields (ϕ) were estimated with data in at least duplicate and coefficients of variation were below 10 %.

Results and Discussion

Comparison of Properties of Readily-Available Fluorophores

For favorable sensitivity of this new homogenous method, the following properties of acceptors in FRET probes are primarily concerned: (a) their rotation freedom in bound probes and thus the angular factor affecting FRET efficiency, (b) the overlapping regions between their excitation peaks and the emission peaks of proteins, (c) their sizes and affinities of the resulting FRET probes, (d) the differences in their emission under the excitation around 335 nm and around 280 nm, (e) their quantum yields in the bound states. The sensitivity to quantify changes of protein fluorescence is primarily determined by the first three factors while that to quantify probe fluorescence is affected by all the five factors. Moreover, the ease to conjugate acceptors with binding moieties for common proteins, the cost and the storage stability of the resulting FRET probes should also be considered.

Many fluorophores have excitation peaks around 335 nm and reasonable sizes to act as candidate acceptors (Fig. 1). Such acceptors display two binding modes in FRET probes of different proteins. BNEDA is a FRET probe of SAV; 1-naphthylamine as the acceptor in BNEDA bound to SAV exhibits an emission peak around 430 nm while free BNEDA in neutral phosphate buffer shows an emission peak around 445 nm [19, 20]. Final 15 % tetrahydrofurane (THF) causes the blue-shift of the emission peak of free BNEDA comparable to that of BNEDA bound to SAV (Fig. 2). Hence, mixtures of organic solvents and neutral phosphate buffer are employed to mimic protein binding sites for the preliminary screening of candidate acceptors.

Excitation spectra of 7-diethylaminocoumarin, 1-naphthylenol and 8-hydroxyquinine in neutral buffer are unfavorable and exhibit tiny changes in mimicked binding sites (Table 1). Excitation peaks of other fluorophores consistently exhibit small red-shifts in binding sites mimicked

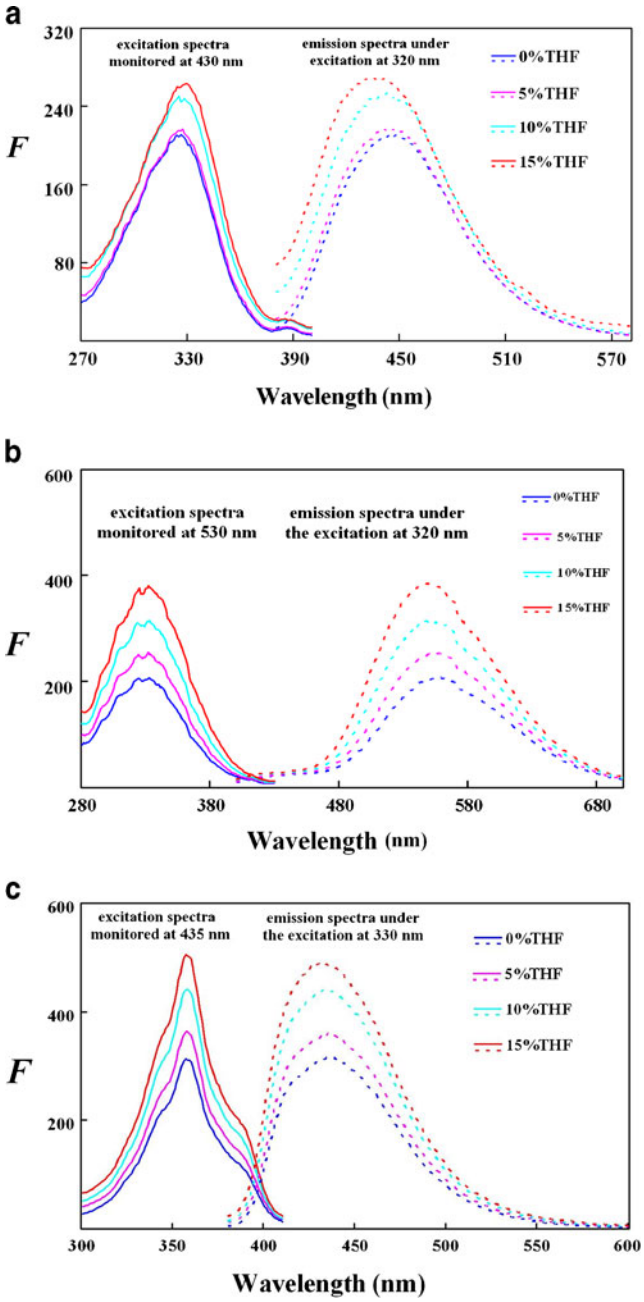

Fig. 2 Effects of THF on fluorescence spectra of representative fluorophores in 10 mM sodium phosphate buffer at pH 7.0 (PBS). **a**. BNEDA at 10 nM. **b**. BDEDA at 10 nM. **c**. BACEDA at 10 nM

with organic solvents (Fig. 2). Hence, most tested fluorophores seem suitable as FRET acceptors to quantify protein fluorescence with this new homogenous method.

Candidate fluorophores show emission peaks with blue-shifts in mimicked binding sites, which is most pronounced with dansylamide. In neutral phosphate buffer, the quantum yields of 1-naphthylamine, 7-hydroxycoumarin, and 9-methylacridine are about 0.70, 0.45 and 0.35, respectively, while those of other tested fluorophores are below 0.25 (Table 2). 2-naphthylenol is an unfavorable acceptor to

Table 1 Effects of THF on excitation properties of candidate fluorophores

Fluorophores	Fluorescence parameters at different levels of THF in sodium phosphate buffer at pH 7.0														
	λ_{ex} (nm)			$F_{ex,\ 330\pm5nm}/F_{ex,\ 280\pm5nm}$			$F_{ex,\ 333\pm5nm}/F_{ex,\ 280\pm5nm}$			$F_{ex,\ max\pm5nm}/F_{ex,\ 280\pm5nm}$					
(THF levels)	0 %	5 %	10 %	15 %	0 %	5 %	10 %	15 %	0 %	5 %	10 %	15 %	0 %	5 %	10 %	15 %
A1	325	327	328	330	2.57	2.10	1.98	1.78	3.27	2.78	2.34	2.22	3.47	3.29	3.02	3.00
A2	324	324	325	325	2.47	2.38	2.32	2.28	2.31	2.25	2.21	2.18	2.60	2.49	2.38	2.32
B1	293	295	295	296	0.15	0.15	0.16	0.18	0.09	0.09	0.10	0.10	1.15	1.15	1.17	1.20
B2	324	324	324	324	0.51	0.56	0.59	0.73	0.38	0.42	0.44	0.56	0.67	0.72	0.75	0.90
C1	323	323	323	323	2.81	2.88	2.97	3.02	2.70	2.78	2.88	2.93	2.93	3.00	3.06	3.10
C2	384	384	384	385	2.36	2.19	2.13	2.10	2.62	2.44	2.39	2.36	8.25	8.34	8.82	9.43
D	327	327	328	329	2.45	1.77	1.54	1.45	2.47	2.20	2.19	1.97	2.53	2.26	2.24	2.00
E1	357	357	357	357	3.52	2.76	2.66	2.43	4.09	3.19	3.06	2.78	8.72	6.68	6.38	5.70
E2	354	355	355	356	4.86	4.40	4.38	4.22	5.84	5.26	5.22	4.99	10.74	9.95	9.83	9.42
F	309	307	307	306	0.87	0.91	0.97	1.02	0.73	0.76	0.81	0.86	1.49	1.52	1.58	1.61

$F_{ex,\ 330\pm5nm}$, $F_{ex,\ 280\pm5nm}$, $F_{ex,\ 333\pm5nm}$, $F_{ex,\ max\pm5nm}$ are the integrated signal from the detection wavelength minus 5 nm to the detection wavelength plus 5 nm because the slit is 10 nm

Table 2 Effects of THF on emission properties of candidate fluorophores

Fluorophores	Emission spectrum parameters at different levels of THF in 10.0 mmol/L sodium phosphate buffer at pH 7.0													
	quantum yield (Φ)			λ_{em} (nm)			$F_{em\pm5nm}/F_{em\ all}$			$\Phi \times (F_{em\pm5nm}/F_{em\ all})$				
(THF levels)	0 %	5 %	10 %	15 %	0 %	5 %	10 %	15 %	0 %	5 %	10 %	15 %	0 %	5 %	10 %	15 %
A1	0.71	0.75	0.83	0.89	443	441	435	431	0.127	0.123	0.113	0.111	0.090	0.092	0.093	0.099
A2	0.68	0.72	0.80	0.81	447	446	443	439	0.101	0.104	0.109	0.117	0.069	0.074	0.087	0.094
B1	0.12	0.13	0.14	0.15	468	468	467	466	0.109	0.108	0.107	0.106	0.013	0.014	0.015	0.016
B2	0.24	0.24	0.25	0.25	411	410	409	407	0.086	0.079	0.074	0.061	0.021	0.019	0.018	0.015
C1	0.45	0.45	0.40	0.37	451	451	451	451	0.154	0.157	0.166	0.173	0.070	0.070	0.067	0.064
C2	0.10	0.10	0.14	0.16	481	480	478	473	0.153	0.153	0.154	0.156	0.015	0.016	0.021	0.025
D	0.04	0.08	0.11	0.15	562	560	555	551	0.081	0.099	0.089	0.089	0.006	0.008	0.010	0.013
E1	0.17	0.18	0.22	0.25	436	436	435	433	0.136	0.138	0.139	0.140	0.023	0.025	0.031	0.034
E2	0.35	0.31	0.25	0.23	448	438	433	430	0.113	0.108	0.098	0.098	0.039	0.034	0.026	0.023
F	0.04	0.05	0.06	0.08	491	491	488	488	0.096	0.092	0.081	0.071	0.004	0.004	0.005	0.006

$F_{em\pm5nm}$ is the integrated signal from the peak wavelength minus 5 nm to the peak wavelength plus 5 nm (emission slit is 10 nm). $F_{em\ all}$ was the integrated signal from 350 nm to 100 nm after the peak of emission.

quantify probe fluorescence because it has two emission peaks (data not given). Mimicked binding sites with THF, methanol, or ethanol below 15 % exert positive effects on quantum yields of dansylamide, acrindine-9-carboxyl acid, and 1-naphthylamine; such a positive effect on the quantum yield of dansylamide is the largest, but its quantum yield is just about 0.15 even in the presence of 15 % THF. At higher THF levels, fluorescence of 1-naphthylamine and acridine-9-carboxyl acid decreases slowly while that of dansylamide continues to increase with larger blue-shifts of emission peaks (data not given). Unfortunately, environments in binding sites mimicked with THF or methanol negatively impact the quantum yield of 9-methylacridine; acetone at 5 % quenches the fluorescence of 1-naphthylamine, and effectively decreases the fluorescence of other tested fluorophores except acridine-9-carboxyl acid (Table 3). For large differences in the emission under the excitation around 335 nm and around 280 nm, 9-methylacridine seems more favorable as the acceptor in FRET probes. However, the ratio of the detected signals (which was indexed by the integrated signals from an emission peak for detection (λ_{em}) minus half of the slit to λ_{em} plus half of the slit) to the total integrated emission (from 350 nm to that equal to λ_{em} plus 130 nm) directly determines the sensitivity for quantifying a FRET probe. Based on such ratios of candidate fluorophores in neutral buffer, 1-naphthylamine ranks the first, 7-hydroxycoumarin stands the second while acridine derivatives are the third (Table 3). Hence, (a) 7-hydroxylcoumarin, acridine-9-carboxyl acid and 1-naphthylamine seem suitable for quantifying probe or protein fluorescence while dansylamide seems suitable for quantifying protein fluorescence only; (b) representative proteins are needed to examine effects of binding modes on their quantum yields.

In general, moieties in ligands bound by proteins can be linked with fluorophores via reactions among carboxyl acid, amino and/or hydroxyl groups. FRET probes with dansylamide as the acceptor can be easily prepared at low cost; 1-naphthylamine is easy to be derivatised for the conjugation with common binding moieties at favorable cost; such two types of FRET probes have reasonable storage stability. Fluorescence of 7-hydroxycoumarin requires its 7-hydroxyl group, but 7-hydroxycoumarin is too hard to be derivatised for conjugating with common binding moieties to prepare FRET probes with 7-hydroxycoumarin as the acceptor. Additionally, methyl group on 9-methylacridine is suitable for the linkage to binding moieties, but all resulting candidate FRET probes display quite low storage stability [31]. However, acridine-9-carboxyl acid is easily conjugated with binding moieties to give intended FRET probes with reasonable storage stability. Hence, 1-naphthylamine, dansylamide and acridine-9-carboxyl acid are tested with representative proteins for their suitability

Table 3 Effects of different organic solvents on quantum yields of FRET probes

conditions	Quantum yield (Φ) of probes in 10 mmol/L sodium phosphate buffer at pH 7.0											
	PBS	THF			Methanol			Ethanol			Acetone	
Probes	0 %	5 %	10 %	15 %	5 %	10 %	15 %	5 %	10 %	15 %	1 %	5 %
BNEDA	0.71	0.75	0.83	0.89	0.74	0.76	0.81	0.76	0.78	0.80	0.179	0.047
BDEDA	0.059	0.064	0.071	0.110	0.062	0.072	0.097	0.061	0.080	0.099	0.046	0.031
BACEDA	0.110	0.118	0.120	0.138	0.123	0.126	0.113	0.138	0.142	0.148	0.128	0.142
DDPDA[a]	0.054	0.066	0.071	0.134	0.055	0.065	0.067	0.061	0.062	0.065	0.046	0.041
NCHEDA	0.72	0.79	0.85	0.86	0.78	0.82	0.84	0.84	0.85	0.88	0.128	0.040

[a] Quantum yield of BDEDA is 0.138 in methanol, and 0.368 in 95 % ethanol

as acceptors in FRET probes and FRET efficiency in the complexes of proteins and such FRET probes.

Fluorescence Properties of Bound Probes, FRET Efficiency and Applications

Glutathione-S-transferase (GST) binds hydrophobic inhibitors inside its active site with low selectivity [25, 26]. Of porcine liver GST π, one tryptophan residue and several tyrosine residues localize inside its active site of diameter within 1.5 nm. Such an active site will provide distances short enough for FRET between a bound acceptor and tryptophan and tyrosine residues inside the active site when all other prerequisites are met (Fig. 3). Series of candidate FRET probes to GST are screened. Among GST inhibitors derivatised from dansylamide and 1-naphthylamine, *N*-(1-naphthyl)-*N*′-cyclohexanylcarbonyl-ethylenediamine (NCHEDA) and didansyl-1,3-propanydiamine (DDPDA) have the inhibition constants of about 4.3 μM and 6.7 μM, respectively, and few other candidate FRET probes of GST display sufficient affinities. On the other hand, SAV has a very small binding site for biotin with excellent selectivity; SAV is rich in tryptophan residues in the vicinity of the binding site for biotin; fluorescent biotin derivatives are ligands to SAV. The acceptors in FRET probes of SAV are localized on SAV surface and thus have high rotation freedom to adjust their orientations with respect to donors [10]. Hence, SAV and GST are used as two representative proteins to test the effects of acceptor binding modes on their quantum yields and FRET efficiency in the complexes with proteins.

The binding of *N*-(biotinyl)-*N*′-(9-acridinyl)-carbonylamide-ethylenediamine (BACEDA) to SAV reduce SAV fluorescence at 335 nm while the complexes display the typical emission peak of BACEDA around 435 nm with an additional excitation peak around 280 nm (Fig. 4). Both the excitation peak and emission peak of the bound BACEDA display negligible differences from those of free BACEDA, respectively. The bound BACEDA has a quantum yield of about 0.20 under excitation at 325 nm, comparable to that at 15 % THF (Table 4). With BACEDA, relative affinities of some biotin derivatives are consistent with those obtained with BNEDA or BDEDA as the FRET probe, respectively (Table 5) [20, 27]. However, the reaction mixtures of GST and tested acridine-9-carboxyl acid derivatives exhibit no detectable changes of emission spectra under the excitation around 280 nm or 335 nm, indicating that there are no complexes formed between GST and such acridine-9-carboxyl acid derivatives. Therefore, acridine-9-carboxyl acid is an effective acceptor in FRET probes when it has sufficient rotation freedom in bound FRET probes and the resulting FRET probes have reasonable affinities.

Free BDEDA exhibits an excitation valley around 280 nm with the emission peak around 545 nm while BDEDA bound

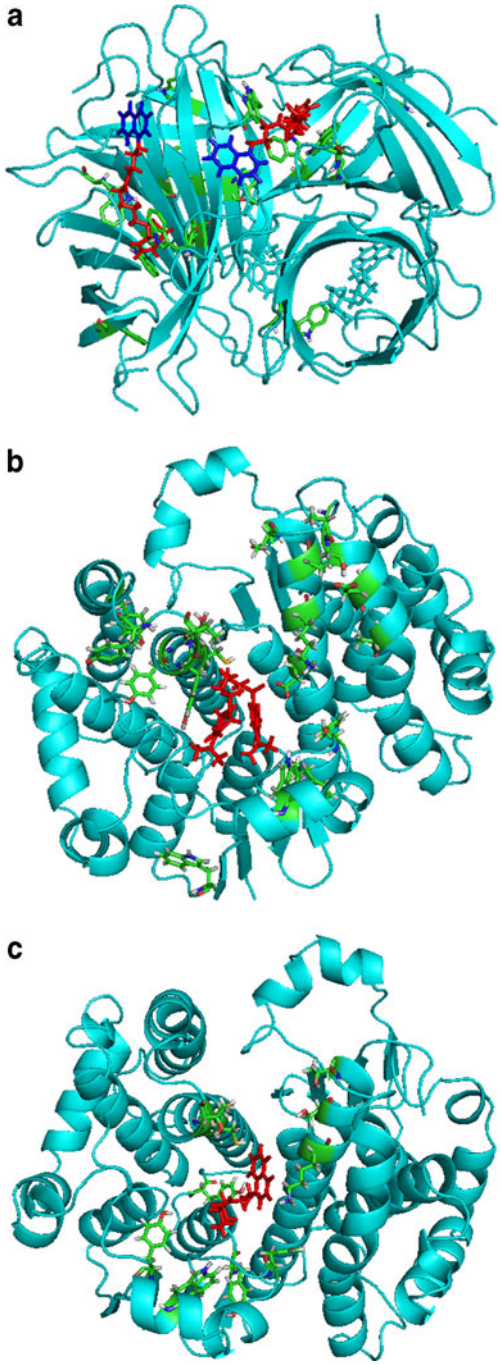

Fig. 3 DDPDA and NCHEDA in GST active site and BNEDA in SAV. **a**. BNEDA in SAV. The ring in blue is 1-naphthylamine that is conjugated with biotin in red. Tryptophan residues are displayed as sticks with carbon atom in green, nitrogen atom in blue while oxygen atom in red. The coordinates for the complexes of SAV and BNEDA are those prepared before [19]. **b**. DDPDA in GST. Tryptophan and tyrosine residues are displayed as sticks with carbon atom in green, nitrogen atom in blue while oxygen atom in red. The molecule in red is DDPDA. Amino acid residues in close proximity are shown. **c**. NCHEDA in GST. Tryptophan and tyrosine residues are displayed as sticks with carbon atom in green, nitrogen atom in blue while oxygen atom in red. The molecule in red is DDPDA. Amino acid residues in close proximity are shown

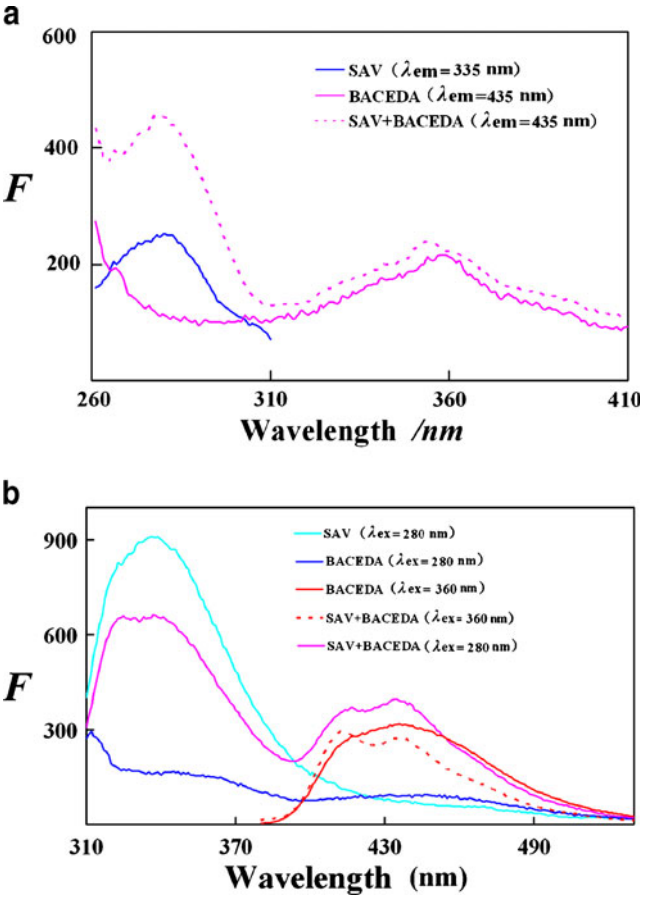

Fig. 4 Fluorescence spectra of BACEDA and its complexes with SAV in the PBS. Final BACEDA and SAV (binding site) are 35 nM and 40 nM, respectively. **a**. Excitation spectra of SAV, BACEDA and their complex. **b**. Emission spectra of SAV, BACEDA and their complex

to SAV has an additional excitation peak close to 280 nm with the emission peak around 520 nm [20]. Under the excitation at 285 nm, the decrease in the emission at 335 nm of complexes of BDEDA and SAV is larger than the increase in the emission of the bound BDEDA around 520 nm. Under the excitation at 285 nm, GST exhibits an emission peak around 335 nm; the reaction mixture of DDPDA and GST exhibits an emission peak around 500 nm higher than that of free DDPDA at 545 nm, but such an increase in the emission around 500 nm is absent for the reaction mixture of SAV and DDPDA. These results support that complexes are formed between GST and DDPDA, but are not formed between SAV and DDPDA. The larger blue-shift of the emission peak of the bound DDPDA indicates that the active site of GST is more hydrophobic than the surface of SAV where dansylamide in BDEDA localizes. The increase in the emission at 500 nm of the complexes of GST and DDPDA is very small while the change of the emission at 335 nm can hardly be detected under the excitation at 285 nm (Fig. 5). Free BDEDA and DDPDA display quantum yields of about 0.04 and 0.06 under the excitation at 325 nm, correspondingly. The quantum yield of DDPDA

Table 4 Quantum yields of FRET probes bound by representative proteins

Probes	Target	Quantum yields (Φ) and quantification sensitivity			
		Free in PBS	Bound (Φ_a) [a]	Bound (Φ_b) [b]	$\Phi_b \times (F_{em\pm5nm}/F_{em\ all})$ [c]
BNEDA	SAV	0.71	0.49	0.49	~0.060
BDEDA	SAV	0.04	0.11	0.11	~0.011
BACEDA	SAV	0.11	0.20	0.20	~0.024
DDPDA	GST	0.06	0.16	~0.27	~0.023
NCHEDA	GST	0.72	0.46	~0.15	~0.018

For each biotin derivative as a probe, its quantum yield in bound state is determined with final 40 nM SAV (binding sites) and 35 nM probe. For DDPDA, its quantum yield in bound state is determined with 4 μM GST (binding sites) and 0.80 μM probe under the excitation slit of 5 nm while emission slit of 10 nm. For NCHEDA, its quantum yield in bound state is determined with 4 μM GST (binding sites) and 0.80 μM probe under the excitation and emission slits of 5 nm

[a] The contributions of free probes are not corrected to give the apparent quantum yield (Φ_a)

[b] Due to extremely high affinities of SAV probes [20], the correction of roles of free probes makes no changes of quantum yields. It is assumed that free probe and bound probe of GST have the same absorbance. The quantum yield of DDPDA is corrected with an inhibition constant of 6.7 μM, while that of NCHEDA is corrected with an inhibition constant of 4.3 μM, to estimate the concentration of bound probe (C_f) and that of free probe (C_b) in reaction mixture. Assigning the quantum yield of a free probe to ϕ_f while that of the bound probe to ϕ_b, the correction is made according to $0.8 \times \Phi_a = C_f \times \phi_f + C_b \times \phi_b$ to estimate ϕ_b

[c] $F_{em\pm5nm}$ is the integrated signal from the peak wavelength minus 5 nm to the peak wavelength plus 5 nm. $F_{em\ all}$ was the integrated signal from 350 nm to 100 nm after the emission peak

bound to GST is about 0.16 when the role of free DDPDA is not corrected, but about 0.27 after the role of free DDPDA is corrected (Table 4). BDEDA bound to SAV has a quantum yield of just about 0.11, but FRET efficiency in its complexes with SAV is much stronger than that in the complexes of DDPDA and GST. These results support that acceptors in FRET probes buried in GST binding sites exert negligible FRET; dansylamide in FRET probes is preferred to be buried inside protein binding sites for higher quantum yield to quantify probe fluorescence, but FRET efficiency in such cases is quite low for this new method. Moreover, homogenous assays of affinities of biotin derivatives with BDEDA to quantify SAV fluorescence are effective [20], but the affinity of DDPDA to GST can not be reliably estimated due to quite small changes of fluorescene after the formation of complexes. Hence, (a) this new method is effective to proteins when acceptors in FRET probes are not buried inside protein binding sites; (b) dansylamide is a suitable acceptor in FRET probes only to quantify protein fluorescence when other criteria are met concurrently.

BNEDA in complexes with SAV exhibits an excitation peak around 280 nm besides that around 325 nm and its emission peak display a small blue-shift from about 445 nm to 430 nm. Under the excitation at 280 nm, the increase in the emission at 430 nm after the binding of BNEDA to SAV is stronger than the decrease in SAV emission at 335 nm. More importantly, BNEDA bound to SAV under the excitation at 280 nm produces stronger emission around 430 nm than free BNEDA under the excitation at 325 nm, and much higher than that of BDEDA bound to SAV under the excitation at 325 nm. BNEDA bound to SAV display a quantum yield that is just about 70 % of free BNEDA, but is much higher than that of the bound BDEDA (Table 4). The use of BNEDA as a FRET probe to SAV gives consistent affinities of some biotin derivatives by quantifying fluorescence of SAV or BNEDA [20]. On the other hand, the reaction mixture of NCHEDA and GST exhibits an excitation peak around 330 nm and an emission peak around 430 nm while no detectable excitation peak around 280 nm (Fig. 6). Under the excitation at 280 nm, there is a decrease in the emission of the reaction mixture of GST and NCHEDA around 430 nm while no detectable change in the emission around 335 nm; this result supports there are complexes formed

Table 5 Estimation of relative affinities of biotin derivatives with BACEDA

Methods	K_X (μM)		K_X/K_A
Reported with BNEDA as the probe	BDETA	188	6.7
	BMPL	82	2.9
	BCHA	28	1
The use of BACEDA as the probe	BDETA	225	5.1
	BMPL	180	2.5
	BCHA	72	1

The dissociation constant of BACEDA is about 30 fM in the PBS at pH 7.0. Final concentrations of BACEDA and SAV in reaction mixtures are 100 nM and 80 nM, respectively. The half-effective concentration of each candidate biotin derivative is estimated as reported before to derive the dissociation constant [19, 20]. Fluorescence is monitored at 435 nm under the excitation at 285 nm. Results were from duplicated assays with CV below 13 %. Biotin derivatives under test are N-biotinyl-diethanolamine (BDETA), N-biotinylmorphiline (BMPL), and N-biotinylcyclohexanylamine (BCHA)

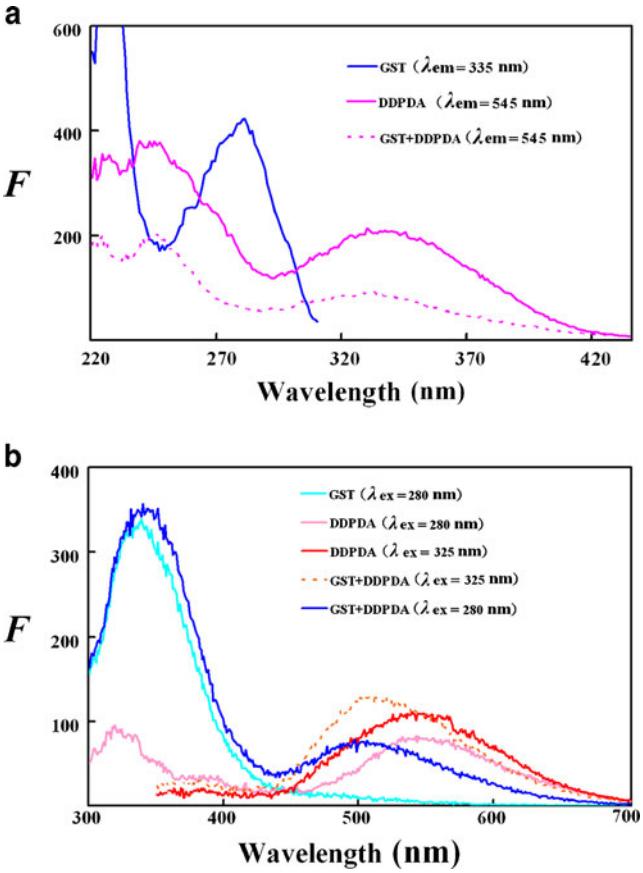

Fig. 5 Fluorescence spectra of DDPDA and its complexes with GST in the PBS. Final DDPDA and GST (binding site) are 0.80 μM and 4.0 μM, respectively. Slit width for excitation is preset at 5 nm while that for emission is still 10 nm. **a**. Excitation spectra of GST, DDPDA and their complex. **b**. Emission spectra of GST, DDPDA and their complex

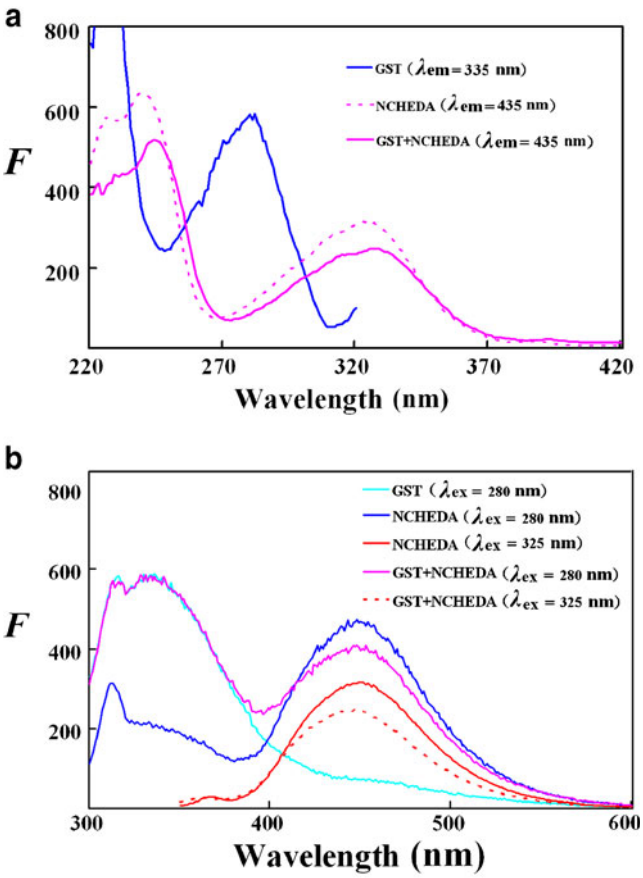

Fig. 6 Fluorescence spectra of NCHEDA and its complexes with GST in the PBS. Final NCHEDA and GST (binding sites) are 0.80 μM and 4.0 μM, respectively. Slit width is preset at 5 nm for both excitation and emission. **a**. Excitation spectra of GST, NCHEDA and their complex. **b**. Emission spectra of GST, NCHEDA and their complex

between GST and NCHEDA but negligible FRET effects in such complexes. Meanwhile, the mixture of SAV and NCHEDA produces no detectable changes of fluorescence around 430 nm or 335 nm. Consequently, the stronger FRET in complexes of SAV and BNEDA should be due primarily to higher rotation freedom of the acceptor in the bound probe and thus a larger angular factor. The quantum yield of the bound NCHEDA is about 0.46 when the role of free NCHEDA is not corrected, but is about 0.15 after the contribution of free NCHEDA is corrected (Table 4). It is reported that 5-aminoquinazoline-2,4-(1 *H*,3 *H*)-dione is an acceptor for tryptophan and tyrosine residues in native proteins with a quantum yield of about 0.40 in neutral buffer [21], but it has multiple groups of similar reactivity that complicate its conjugation with moieties bound by proteins. Hence, (a) 1-naphthylamine in FRET probes is a practical acceptor to quantify the emission of probes or proteins when it is not buried inside binding sites; (b) an acceptor is more favorable if it has quantum yield higher than that of 1-naphthylamine in bound FRET probes but smaller than that of 1-naphthylamine in free probes.

Taken together, this new method is applicable to proteins that do not bury acceptors of their FRET probes inside protein binding sites. Due to hydrophobicity of common acceptors for tryptophan/tyrosine residues, this new homogenous method is inapplicable to proteins bearing low selectivity for hydrophobic ligands. For any protein of high selectivity for its ligands, however, a suitable acceptor should be carefully linked to a proper position of its binding moiety so that the acceptor in the FRET probe can be localized on protein surface rather than be buried inside protein binding site. In general, 1-naphthylamine is a suitable acceptor for quantifying its fluorescence when it is not buried inside protein binding sites; dansylamide buried inside protein binding sites has high quantum yield, but FRET efficiency in this case is usually negligible.

Conclusions

To apply this new type of homogenous bioaffinity analysis to proteins that do not bury acceptors of their FRET probes inside binding sites, (a) 1-naphthylamine is a practical acceptor in FRET probes for quantifying the emission of either probes or proteins; (b) dansylamide is an effective acceptor in FRET probes to quantify protein fluorescence; (c) any fluorophore is more favorable when its quantum yield in environments of protein surfaces is higher than that of 1-naphthylamine while its quantum yield in free probes is smaller than that of 1-naphthylamine.

Acknowledgments Supports were from the National Natural Science Foundation of China (no. 81071427), "863" high-technology-program (2011AA02A108), Program for New Century Excellent Talent in University (NCET-09-0926), Natural Science Foundation Project of CQ (CSTC2011BA5039) and Chongqing Education Commission (no. KJ100313).

References

1. Eggeling C, Brand L, Ullmann D, Jager S (2003) Highly sensitive fluorescence detection technology currently available for HTS. Drug Discov Today 8:632–641
2. Sorme P, Kahl-Knutssun B, Huflejt M, Nilsson UJ, Lefler H (2004) Fluorescence polarization as an analytical tool to evaluate galectin-ligand interactions. Anal Biochem 334:36–47
3. Smith DS, Eremin SA (2008) Fluorescence polarization immunoassays and related methods for simple, high-throughput screening of small molecules. Anal Bioanal Chem 391:1499–1507
4. Huang X, Aulabaugh A (2009) Application of fluorescence polarization in HTS assays. Method Mol Biol 565:127–143
5. Shen Y, Hu Y, Chen B, Yao S (2010) Screening of enzyme inhibitors from traditional Chinese medicine. Comb Chem High T Scr 13:885–899
6. Uri A, Lust M, Vaasa A, Lavogina D, Viht K, Enkvist E (2010) Bisubstrate fluorescent probes and biosensors in binding assays for HTS of protein kinase inhibitors. Biochim Biophys Acta 1804:541–546
7. Hakamata W, Kurihara M, Okuda H, Nishio T, Oku T (2009) Design and screening strategies for alpha-glucosidase inhibitors based on enzymological information. Curr Top Med Chem 9:3–12
8. Bazin H, Preaudat M, Trinquet E, Mathis G (2001) Homogeneous time resolved fluorescence resonance energy transfer using rare earth cryptates as a tool for probing molecular interactions in biology. Spectrochim Acta A Mol Biomol Spectrosc 57:2197–2211
9. Ohiro Y, Arai R, Ueda H, Nagamune T (2002) A homogeneous and noncompetitive immunoassay based on the enhanced fluorescence resonance energy transfer by leucine zipper interaction. Anal Chem 74:5786–5792
10. Boute N, Jockers R, Issad T (2002) The use of resonance energy transfer in high-throughput screening: BRET versus FRET. Trends Pharmacol Sci 23:351–354
11. Scholes GD (2003) Long-range resonance energy transfer in molecular systems. Ann Rev Phys Chem 54:57–87
12. Milligan G (2004) Applications of bioluminescence- and fluorescence resonance energy transfer to drug discovery at G protein-coupled receptors. Eur J Pharmaceut Sci 21:397–405
13. Miller JM (2005) Fluorecence energy transfer methods in bioanalysis. Analyst 130:265–270
14. Sapsford KE, Berti L, Medintz IL (2006) Materials for fluorescence resonance energy transfer analysis: beyond traditional donor-acceptor combinations. Angew Chem Int Ed 45:4562–4589
15. Gunther JR, Du Y, Rhoden E, Lewis I, Revennaugh B, Moore TW, Kim SH, Dingledine R, Fu H, Katzenellenbogen JA (2009) A set of time-resolved fluorescence resonance energy transfer assays for the discovery of inhibitors of estrogen receptor-coactivator binding. J Biomol Screen 14:181–193
16. Lakowicz JR (2006) Principle of fluorescence spectroscopy, 3rd edn. Springer, Berlin
17. González-Jiménez J, Cortijo M (2004) Resonance energy transfer between tryptophan-214 in human serum albumin and acrylodan, prodan, and promen. Protein J 23:351–355
18. Das P, Mallick A, Haldar B, Chakrabarty A, Chattopadhyay N (2007) Fluorescence resonance energy transfer from tryptophan in human serum albumin to a bioactive indoloquinolizine system. J Chem Sci 119:77–82
19. Liao F, Xie YL, Yang XL, Deng P, Chen YW, Xie GM, Zhu S, Liu BZ, Yuan HD, Liao J, Zhao YS, Yu MA (2009) Homogeneous noncompetitive assay of protein via Förster-resonance-energy-transfer with tryptophan residue(s) as intrinsic donor(s) and fluorescent ligand as acceptor. Biosens Bioelectron 25:112–117
20. Xie YL, Yang XL, Pu J, Zhao YS, Zhang Y, Xie GM, Zheng J, Yuan HD, Liao F (2010) Homogeneous competitive assay of ligand affinities based on quenching fluorescence of tyrosine/tryptophan residues in a protein via Fŏrster-resonance-energy-transfer. Spectrochim Acta A Mol Biomol Spectrosc 77:869–876
21. Xie Y, Maxson T, Tor Y (2010) Fluorescent ribonucleoside as a FRET acceptor for tryptophan in native proteins. J Am Chem Soc 132:11896–11897
22. Wilchek M, Bayer EA, Livnah O (2006) Essentials of biorecognition: the (strept)avidin–biotin system as a model for protein–protein and protein–ligand interaction. Immunol Lett 103:27–32
23. Laitinen OH, Nordlund HR, Hytonen VP, Kulomaa MS (2007) Brave new (strept)avidins in biotechnology. Trends Biotechnol 25:269–277
24. Mitchell FL, Marks GE, Bichenkova EV, Douglas KT, Bryce RA (2008) Molecular probes: insights into design and analysis from computational and physical chemistry. Biochem Soc Trans 36:46–50
25. Dirr HW, Ma K, Huber R, Ladenstein R, Reinemer P (1991) Class Pi: glutathione S-transferase from pig lung, purification, biochemical characterization, primary structure and crystallization. Eur J Biochem 196:693–698
26. Reinemer P, Dirr HW, Ladenstein R, Schäffer J, Gallay O, Huber R (1991) The three-dimensional structure of class pi glutathione Stransferase in complex with glutathione sulfonate at 2.3 A resolution. EMBO J 10:1997–2005
27. Yang XL, Xie YL, Pu J, Zhao H, Liao J, Yuan YH, Zhu S, Long GB, Zhang C, Yuan HD, Chen YW, Liao F (2011) Estimation of affinities of ligands in mixtures via magnetic recovery of target-ligand complexes and chromatographic analyses: chemometrics and an experimental model. BMC Biotechnol 11:44
28. Yang XL, Pu J, Zhao H, Li XY, Liao J, Xie YL, Zhu S, Long GB, Yuan YH, Liao F (2012) Method to screen aromatic ligands in mixtures for quantitative affinities to target using magnetic separation of bound ligands along with HPLC and UV photometry detection. Microchimica Acta 176:243–249
29. Ma LH, Wen ZC, Lin LR, Jiang YB (2001) Dual fluorescence of naphthylamines in alkaline aqueous solution. Chem Phys Lett 346:423–429
30. Ray D, Nag A, Jana A, Goswami D, Bharadwaj PK (2010) Coumarin derived chromophores in the donor-acceptor-donor format that gives fluorescence enhancement and large two-photon activity in presence of specific metal ions. Inorg Chim Acta 363:2824–2832
31. Whitelock HW, Digenis GA (1964) An oxidative amine fragmentation. Tetrahydr Lett 5:521–1524